Studies on the Light-Induced Phase Transition of CsPbBr₃ Metal Halide Perovskite Materials

Chenyu Cao, Shaoming Xue, Fangchao Liu, Qiaoqian Wu, Jialin Wu, Zhenkui Zhang, ChengBo Guan, Wei-Yan Cong, and Ying-Bo Lu*

Cite This: ACS Omega 2023, 8, 20096−20101

Read Online

ACCESS | Metrics & More | Article Recommendations

ABSTRACT: We investigate the internal mechanism of the light-induced phase transition of CsPbBr₃ perovskite materials via density functional theory simulations. Although CsPbBr₃ tends to appear in the orthorhombic structure, it can be changed easily by external stimulus. We find that the transition of photogenerated carriers plays the decisive role in this process. When the photogenerated carriers transit from the valence band maximum to conduction band minimum in the reciprocal space, they actually transit from Br ions to Pb ions in the real space, which are taken away by the Br atoms with higher electronegativity from Pb atoms during the initial formation of the CsPbBr₃ lattice. The reverse transition of valence electrons leads to the weakening of bond strength, which is proved by our calculated Bader charge, electron localization function, and integral value of COHP results. This charge transition releases the distortion of the Pb−Br octahedral framework and expands the CsPbBr₃ lattice, providing possibilities to the phase transition from the orthorhombic structure to tetragonal structure. This phase transition is a self-accelerating positive feedback process, increasing the light absorption efficiency of the CsPbBr₃ material, which is of great significance for the widespread promotion and application of the photostriction effect. Our results are helpful to understand the performance of CsPbBr₃ perovskite under a light irradiation environment.
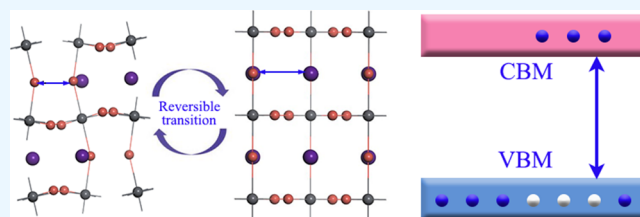
1. INTRODUCTION

Halide perovskites have been widely used in the field of optoelectronics in recent years, due to their high absorption coefficient, high carrier mobility, long carrier lifetime, etc.[1−6] In particular, solar cells using MAPbI₃ and FAPbI₃ as light absorbers have attracted widespread attention, because their efficiencies explosively increase from 3.8% to more than 26.1% in a few years.[7] Meanwhile, halide perovskites are also potential working materials for LEDs,[8] high-energy detector devices,[9] etc. When halide perovskites are utilized in these optoelectronics fields, they always work in the circumstances with light illuminations. Thus, their performances under illumination are critical for the real applications. Therefore, extensive investigations are carried out for this. Lots of interesting light-induced phenomena are discovered for halide perovskites accordingly, for instance, the photostriction effect.

The photostriction effect refers to the light-induced nonthermal crystalline change, which has been reported in many photoelectronic materials, such as BiFeO₃,[10,11] DBTTF-C60,[12] CaCu₃Ti₄O₁₂,[13] PLZT,[14] etc. The photostriction effects were also widely found in perovskite materials. For example, Bi₀.₅Na₀.₅TiO₃ exhibits a remarkable photostriction response under visible light irradiation.[15] A giant light-induced deformation was recently observed in MAPbI₃ with the measured linear strain of approximately 0.72−0.43% under

532 nm illumination.[16] Some studies have shown that the photostriction effect shows an important impact on the physical properties of perovskite materials,[17] e.g., it can improve the charge separation and hinder the subsequent recombination in perovskite materials.[18−21] Thus the photostriction phenomena observed in MAPbI₃[22] and MAPbBr₃[23] pave the way for their widespread applications in optomechanical devices, such as photostriction actuators,[24,25] energy harvesting devices, etc.[26] However, there are still many controversies about the photostriction effect. For example, some researchers believe that the lattice expansion caused by light is completely due to thermal effects and does not require any photo-carrier based mechanism.[27]

Nevertheless, the mechanisms accounting for the light-induced deformation are complex and diverse. The inverse voltage response has been proposed in photomodulated photovoltaic compounds,[28] while the photoisomerization-induced volume change is considered in organic polymers,[28]

and the excessive electron−hole pair-driven deformation is adopted to explain the photostriction effect in nonpolar semiconductors.[29] Studies have shown that the photostriction effect of organic−inorganic hybrid halide perovskite materials results from the photovoltaic effect and the translational symmetry loss of the organic molecular configuration. Meanwhile, similar photon-induced size changes were observed in pure inorganic $CsPbBr_3$ perovskites.[30] Xue et al. found that the $CsPbBr_3$ single crystal undergoes a volume expansion of 3×10^{-5} stimulated by the above-bandgap illumination.[31] More interestingly, a reversible phase transition between the orthorhombic phase and the tetragonal phase generated by the light irradiation is revealed by the XRD measurement, which shows a rapid response (<0.5 s).[31] As reported previously, $CsPbBr_3$ perovskites show complex crystalline structures in various reports, i.e., cubic and monoclinic structures etc.[32,33] And the crystal structures of $CsPbBr_3$ are modulated by external stimulus easily, such as fabrication method, process procedure and impurity doping, etc.[30,32] However, the illumination-induced phase transition is a new light-induced physical effect, which is merely observed in other halide perovskites. Thus, new questions arise from these observations, i.e., the contributions to the light-induced lattice deformation origins from the light-induced phase transition or just a light-induced volumetric change caused by other reactions? How to explain the observed phase transition?

Therefore, this light-induced phase transition phenomenon should be examined and studied in detail. In previous studies, researchers have found that $CsPbBr_3$ perovskite transforms from an orthorhombic phase to tetragonal phase under light irradiation.[31] Thus in this article, we perform a series of theoretical investigations to reveal the mechanism of the phase transition of $CsPbBr_3$ perovskites between the orthorhombic structure and the tetragonal structure. We find that when $CsPbBr_3$ perovskite is illuminated, electrons transition from the valance band maximum (VBM) to the conduction band minimum (CBM). This weakens the bond strength of the Pb−Br−Pb bond and thus changes the Pb−Br−Pb bonding angles and the energetic state of the crystalline systems, which contribute to the light-induced geometric variation and thus the phase transition. Our results can help to put forward the application of photostriction effect and also can improve the physical performance of the halide perovskites.

2. CALCULATION METHODS

We perform density functional theory (DFT) calculations using the Vienna Ab initio simulation package,[34] the exchange-correlation effects are treated in the generalized gradient approximation with the Perdew−Burke−Ernzerhof[35] potential. The core electrons are represented by the projector-augmented wave method.[36] A plane wave cutoff of 400 eV is used to ensure a good convergence in energy. All atoms are fully relaxed without symmetry constraints until convergence to 10^{-4} eV in total energy and 0.01 eV/Å in the force. The Brillouin-zone integrations are performed using $2 \times 2 \times 2$ and $4 \times 4 \times 3$ Monkhorst−Pack grids in the orthorhombic structure and the tetragonal structure, respectively. We use the LOBSTER[37] code to analyze the chemical-bonding interactions, in which the orbitals included are (1) 4s and 4p for Br; (2) 5s, 5p and 6s for Cs; (3) 5d, 6s and 6p for Pb.

3. RESULTS AND DISCUSSION

3.1. Geometric Structures. Although the $CsPbBr_3$ material can be synthesized in several crystal structures, we only pick two structures, i.e., the orthorhombic and the tetragonal structures which are only considered in the previously reported reverse light-induced phase transition. The optimized orthorhombic and tetragonal structures of $CsPbBr_3$ are illustrated in Figure 1, in which the lattice
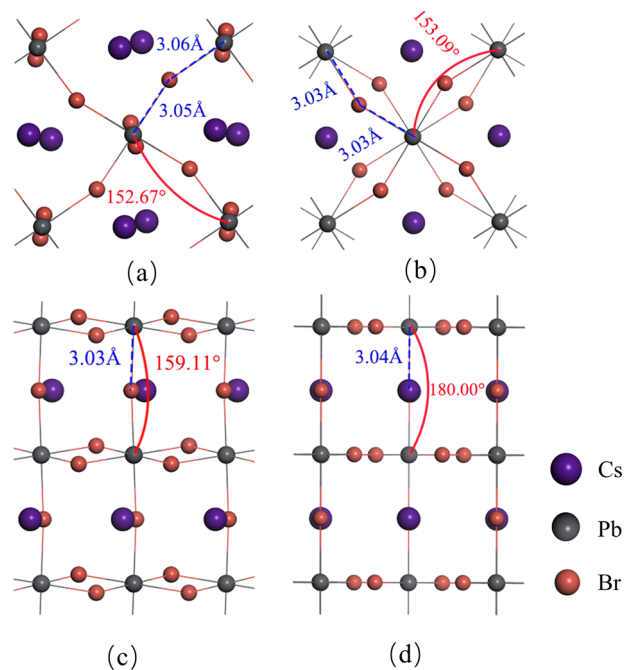

Figure 1. Optimized geometric structures of $CsPbBr_3$ in orthorhombic and tetragonal phases. (a) and (c) are the top and side views of the orthorhombic structure, respectively. (b) and (d) are the top and side views of the tetragonal structure, respectively. Numbers in all figures represent the bond lengths and bond angles, respectively.

parameters of orthorhombic and tetragonal structures are $a = 8.54$ Å, $b = 11.93$ Å, $c = 8.23$ Å and $a = b = 8.33$ Å, $c = 12.15$ Å, respectively. It can be seen that although these two crystal structures are both distorted lattices, they show some obvious different characters. From the top views in Figure 1a,b, we can see that the in-plane Pb−Br−Pb bond angle in the orthorhombic structure is twisted in value of 152.67°, which is lower than the value of 153.09° in the tetragonal structure. Figure 1c,d show that the out-of-plane Pb−Br−Pb bond angle in orthorhombic structure is 159.11°, which is much lower than the value of 180.00° in the tetragonal structure. This means that the distortion of the $PbBr_6$ octahedron in the orthorhombic phase is more severe than that in the tetragonal phase. That is, if $CsPbBr_3$ perovskite transits from the orthorhombic phase to the tetragonal phase, the distortion and the twisting of the $PbBr_6$ octahedra are released, and thus push the lattice outward to expand the whole lattice.

Furthermore, we calculate the total energies of these two $CsPbBr_3$ structures to analyze their formation process. The total energies of $CsPbBr_3$ unit cells in the orthorhombic structure and the tetragonal structure are −16.11 and −16.09 eV, respectively. Compared with the case in tetragonal phase, the lower energy of the orthorhombic structure indicates that the orthorhombic $CsPbBr_3$ system is easier to form under normal conditions, which is consistent with the experimentally

observed phenomenon. However, the energetic difference between these structures is low, thus the external stimulus can change the normal structure easily and give rise to the phase transition between the orthorhombic and tetragonal structure. That is, when $CsPbBr_3$ is illuminated by the light with high enough photon energy, it is very likely to change from the orthorhombic structure to the tetragonal structure, i.e., the light-induced phase transition. As mentioned above, when this phase transition appears, the distortion of the $CsPbBr_3$ lattice will be released and the whole lattice tends to expand, which is exhibited by the experimentally observed light-induced lattice dilation.

3.2. Electronic Structures.
As aforementioned, the photostriction effect is a light-induced physical phenomenon, and it is only experimentally observed when some materials are irradiated by the above-bandgap light. So, the electronic structures of these materials and the subsequently electron excitations are the key points in deep understanding to the intrinsic mechanism of the photostriction effect. Figure 2a,b
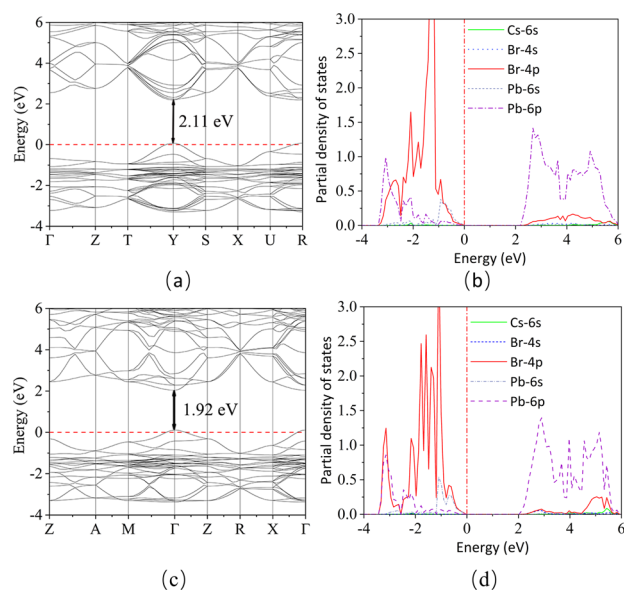
Figure 2. (a) and (b) are the band structure and DOS of $CsPbBr_3$ perovskite in the orthorhombic structure, respectively. (c) and (d) are those properties of $CsPbBr_3$ in the tetragonal structure. The red dashed lines represent the Fermi levels.

shows the band structures and the density of states (DOS) of $CsPbBr_3$ in the orthorhombic phase, which is the ground state under normal conditions. It can be seen that the CBM and the VBM are located at the same position in k-space, which means that the orthorhombic $CsPbBr_3$ is a typical direct band gap semiconductor with the band gap of 2.11 eV, which agrees well with the experimental observations.[38,39] As shown in the partial DOS of the $CsPbBr_3$ perovskite in Figure 2b, the VBM is generated predominantly by Br 4p orbitals, with minor contributions from Pb 6s orbitals. While the CBM originates mainly from Pb 6p orbitals, with minor contributions from Br 4s orbitals. We can see that the contributions from Cs atoms to the band edge are negligible, which is similar of the case in other perovskites. The major function provided by Cs ion is the charge balance for Pb−Br frameworks to maintain the stability of the perovskite structure.

When $CsPbBr_3$ perovskite is irradiated by the above-bandgap light, the photoelectronic effect arises to yield the

light induced carriers, which are excited from VBM to CBM. As illustrated by the electronic structures, the VBM and CBM of $CsPbBr_3$ are predominantly contributed by the Br 4p and Pb 6p orbitals, respectively. That is, when the light induced carriers transit form VBM to CBM, they actually transfer from Br ions to Pb ions, which are taken away by the Br atoms with higher electronegativity from Pb atoms during the initial formation of the $CsPbBr_3$ lattice. It also means that the valence electrons will migrate back from Br ions to Pb ions partially, weakening the bonding strength of Pb−Br bonds. Therefore, we analyze the charge distribution and the bonding interaction to get a deep understanding about this. The calculated Bader charges for each component of $CsPbBr_3$ are shown in Table 1.

Table 1. Distributions of Bader Charges in $CsPbBr_3$ with the Units of Those Values of Unit Charge e

phase	Cs	Pb	Br
orthorhombic	−0.861	−1.140	0.669
tetragonal	−0.868	−1.131	0.668

The Bader charges of Pb and Br ions are quite different from their formal values, indicating the complex bonding interactions composed of ionic and covalent interaction between Pb and Br ions. At the same time, the number of charges on Br/(Pb) ions in the orthorhombic structure is more than/(less than) that in the tetragonal structure. This is consistent qualitatively with our assumption, i.e., if the electrons are excited by light and transit from Br ions back to Pb ions, it is accompanied by the phase transition from the orthorhombic phase to the tetragonal phase.

The electron localization function (ELF) is another means to study the distributions and localizations of the electrons during the formation of the crystalline structures. The ELF can give the measure of electron probability in the field of reference electrons with the same spin and fixed point as well as describe the localization of electrons in lattice space. Figure 3 shows the ELF of these two $CsPbBr_3$ structures, from which
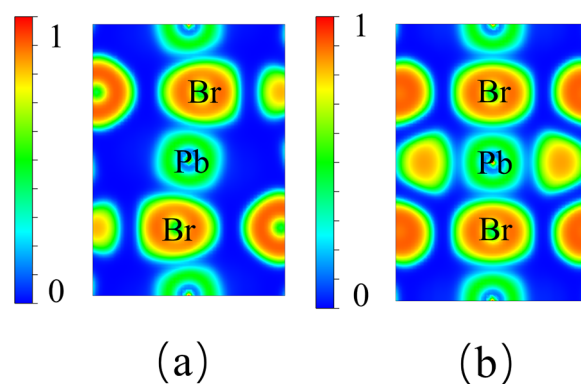

Figure 3. ELF contour plots for $CsPbBr_3$ in (a) orthorhombic and (b) tetragonal phases, respectively.

we can see that in both cases, the charges around Br ions show a more localized character, resulting from the strong electronegativity of Br ions. The crystal orbital Hamilton population (COHP) can represent the local chemical-bonding properties in periodic systems phenomenologically. The integral value of COHP (ICOHP) below the Fermi level can be understood as the numbers of bonding electrons shared between two atoms, it describes the magnitude of the bond

strength qualitatively. The calculated ICOHP for CsPbBr$_3$ in two phases are shown in Table 2 and Figure 4a,b. We calculate

Table 2. Average ICOHP of Pb−Br Bonds for CsPbBr$_3$ Perovskites

phase	no. of bonds	ave.(−ICOHP) [eV]
orthorhombic	8	−1.64
tetragonal	8	−1.62
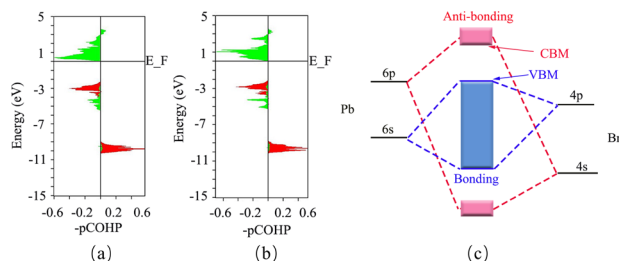
Figure 4. Crystal orbital Hamilton population (COHP) analyses for the Br−Pb bonds of CsPbBr$_3$ perovskite in (a) orthorhombic and (b) tetragonal phases, respectively. The left and right sides represent the antibonding and the bonding states, respectively. The red and the green represent the coupling interactions for Br−4p orbital with Pb−6s orbital and Pb−6p with Br−4s orbitals, respectively. (c) represents the bonding interaction near the band edge of the CsPbBr$_3$ system.

eight Pb−Br bonds in the side view direction for both structures. The average ICOHP of orthorhombic and tetragonal structures is −1.64 and −1.62 eV, respectively. Because the larger absolute value of ICOHP means the stronger bonding interactions, our calculated results show that the Pb−Br bond in the orthorhombic structure is stronger than that in the tetragonal structure. In other words, the bond strength of the Pb−Br bond is weakened after the phase transition from orthorhombic to tetragonal structures. Combined with the calculated results of Bader charge, ELF and ICOHP, we can say that when CsPbBr$_3$ perovskites change the crystalline structure from the orthorhombic phase to tetragonal phase, it is accompanied by the charge transition from Br ions to Pb ions, and the charge density around the Br ions decreases, indicating that the Pb−Br bonds weaken accordingly.

According to the discussions mentioned above, when CsPbBr$_3$ perovskite undergoes the light-induced phase transition, the geometric structure and the bonding inter-actions change evidently, which are believed to bring about evitable change of the electronic structure. From the band structures illustrated in Figure 2c, we can see that the band gap of CsPbBr$_3$ in the tetragonal structure is slightly lower than that in the orthorhombic structure, conforming to the general law of perovskite materials, i.e., with the enhancement of the distortion of the metal octahedra in perovskites, the band gap increases.[40] As shown in Figure 4c, we know that the VBM of CsPbBr$_3$ is formed by the antibonding state ascribed to the coupling of Pb−6s and Br−4p orbitals. And the CBM is the antibonding state coupled by Pb−6p and Br−4s orbitals. Moreover, we noticed that the volume of the orthorhombic structure is 838.60 Å^3, and the volume of the tetragonal structure is 843.55 Å^3. That is, if CsPbBr$_3$ transforms from orthorhombic to tetragonal phase, the lattice expansion leads to the weakening of the twisting and rotation of the PbBr$_6$ octahedron, the increase of the Pb−Br−Pb bond angle and the

decrease of the lateral displacement between the Pb and Br atoms, as shown in Figure 1. This enhances the s-p orbital coupling between Pb and Br atoms,[41] so both VBM and CBM (all antibonding states) shift upward. The volume deformation potentials are often used to express the relationship between the volume change and the shift of band edge, which is inversely proportional to the energy difference between the two atomic orbitals of bonding interactions.[42] The energy difference between Br−4p and Pb−6s is lower than that between Br−4s and Pb−6p, so the VBM has a higher volume deformation potential than the CBM. Namely, the VBM is more sensitive to changes of the coupling interactions and shift with a higher value, so to reduce bandgap.

Combined with the above studies, we know that illumination could stimulate CsPbBr$_3$ to transform from an orthorhombic to a tetragonal phase with a concomitant reduction in the band gap. Furthermore, if the band gap of CsPbBr$_3$ perovskite decreases, it could absorb more light, which will strengthen the light-induced phase transition of CsPbBr$_3$ perovskite further. Then the higher phase transition results to a lower average band gap, which in turn lead to the greater light absorption. Therefore, the photostriction effect of the CsPbBr$_3$ material is a self-accelerating positive feedback process, and this self-accelerating process increases the light absorption efficiency of the CsPbBr$_3$ material, which is of great significance for the widespread promotion and application of the photostriction effect.

4. CONCLUSIONS

By a series of first-principles approaches, we investigate the possibilities of light-induced phase transition of CsPbBr$_3$ perovskite from the orthorhombic structure to the tetragonal phases elaborately. The calculated total energies show that CsPbBr$_3$ perovskite tends to appear in the orthorhombic structure under normal conditions, for the lower energetic state. However, it may be stimulated by external factors easily to transform to the tetragonal phase, such as it is irradiated by light with sufficient photon energy. When this material indeed transforms from the orthorhombic phase to the tetragonal phase after illumination, the distortion of the PbBr$_6$ octahedron is released, leading the lattice to expand outward, which accounts for the experimentally observed light-induced lattice dilation. Via analyses of the electronic structures, we find that the CBM and VBM are mainly distributed on Pb ions and Br ions, respectively. That is, when the photogenerated carriers transit from the VBM to CBM in the reciprocal space, they actually transit from Br ions to Pb ions in real space, which are taken away by the Br atoms with higher electronegativity from Pb atoms during the initial formation of the CsPbBr$_3$ lattice. Thus, the backward transition of the valence electrons weakens the strength of Pb−Br bonds, which is proved by our calculated Bader charge, ELF, and ICOHP results. The weakening of Pb−Br bonds releases the twisting of the Pb−Br frameworks and expands the lattice, giving birth to the phase transition from orthorhombic to the tetragonal structures, which agrees well with our geometric and energetic discussions. At last, we find that the photostriction effect of CsPbBr$_3$ material is a self-accelerating positive feedback process. Thus we make clear the intrinsic mechanism of light-induced phase transition for CsPbBr$_3$ perovskites. As the geometric structures determine the physical properties of optoelectronic materials, so our findings are useful to

understand the performances of CsPbBr$_3$ perovskites when they work under light irradiation circumstances.

AUTHOR INFORMATION

Corresponding Author

Ying-Bo Lu − *School of Space Science and Physics, Shandong University, Weihai 264209, China;* ● orcid.org/0000-0001-7799-8751; Email: lyb@sdu.edu.cn

Authors

Chenyu Cao − *School of Space Science and Physics, Shandong University, Weihai 264209, China;* ● orcid.org/0000-0002-7886-6950

Shaoming Xue − *School of Space Science and Physics, Shandong University, Weihai 264209, China*

Fangchao Liu − *School of Space Science and Physics, Shandong University, Weihai 264209, China*

Qiaoqian Wu − *School of Space Science and Physics, Shandong University, Weihai 264209, China*

Jialin Wu − *School of Space Science and Physics, Shandong University, Weihai 264209, China*

Zhenkui Zhang − *School of Science, Langfang Normal University, Langfang 065000, China*

ChengBo Guan − *School of Space Science and Physics, Shandong University, Weihai 264209, China*

Wei-Yan Cong − *School of Space Science and Physics, Shandong University, Weihai 264209, China*

Complete contact information is available at:
https://pubs.acs.org/10.1021/acsomega.3c02378

Notes

The authors declare no competing financial interest.

ACKNOWLEDGMENTS

REFERENCES

(1) Yu, F. *Internal Polarization Effect in Perovskite Solar Cells.* Master's Thesis ; University of Pittsburgh, 2015.

(2) Eperon, G. E.; Paternò, G. M.; Sutton, R. J.; Zampetti, A.; Haghighirad, A. A.; Cacialli, F.; Snaith, H. J. Inorganic caesium lead iodide perovskite solar cells. *J. Mater. Chem. A* 2015, *3*, 19688−19695.

(3) Evolution of Perovskite Photovoltaics and Decrease in Energy Payback Time. *J. Phys. Chem. Lett.* 2013, *4* (), 3733−3734, DOI: 10.1021/jz402141s.

(4) Ling, Y.; Yuan, Z.; Tian, Y.; Wang, X.; Wang, J. C.; Xin, Y.; Hanson, K.; Ma, B.; Gao, H. Bright Light-Emitting Diodes Based on Organometal Halide Perovskite Nanoplatelets. *Adv. Mater.* 2016, *28*, 305−311.

(5) Kuang, D. B.; Klein, C.; Zhang, Z. P.; Ito, S.; Moser, J. E.; Zakeeruddin, S. M.; Gratzel, M. Stable, high-efficiency ionic-liquid-based mesoscopic dye-sensitized solar cells. *Small* 2007, *3*, 2094−2102.

(6) Peng, G.; Graetzel, M.; Nazeeruddin, M. K. Organohalide lead perovskites for photovoltaic applications. *J. Phys. Chem. Lett.* 2014, *7*, 2448−2463.

(7) Mir, W. J.; Sheikh, T.; Arfin, H.; Xia, Z. G.; Nag, A. Lanthanide doping in metal halide perovskite nanocrystals: spectral shifting, quantum cutting and optoelectronic applications. *NPG Asia Mater.* 2020, *12*, 9.

(8) Sk, M. Recent progress of lead-free halide double perovskites for green energy and other applications. *Appl. Phys. A* 2022, *128*, 462.

(9) Zhou, Y.; Chen, J.; Bakr, O. M.; Mohammed, O. F. Metal Halide Perovskites for X-ray Imaging Scintillators and Detectors. *ACS Energy Lett.* 2021, *6*, 739−768.

(10) Kundys, B.; Viret, M.; Colson, D.; Kundys, D. O. Light-induced size changes in BiFeO3 crystals. *Nat. Mater.* 2010, *9*, 803−805.

(11) Paillard, C.; Xu, B.; Dkhil, B.; Geneste, G.; Bellaiche, L. Photostriction in ferroelectrics from density functional theory. *Phys. Rev. Lett.* 2016, *116*, No. 247401.

(12) Zhang, Z.; Remsing, R. C.; Chakraborty, H.; Gao, W.; Yuan, G.; Klein, M. L.; Ren, S. Light-induced dilation in nanosheets of charge-transfer complexes. *Proc. Natl. Acad. Sci. U. S. A.* 2018, *115*, 3776−3781.

(13) Li, X.; Chen, C.; Zhang, F.; Huang, X.; Yi, Z. Giant photostriction of CaCu3Ti4O12 ceramics under visible light illumination. *Appl. Phys. Lett.* 2020, *116*, No. 112901.

(14) Chen, C.; Li, X.; Lu, T.; Liu, Y.; Yi, Z. Reinvestigation of the photostrictive effect in lanthanum-modified lead zirconate titanate ferroelectrics. *J. Am. Ceram. Soc.* 2020, *103*, 4074−4082.

(15) Fang, H. L.; Chen, C.; Zhang, F. Q.; Cao, M. H.; Yi, Z. G. Significant photostrictive response in lead-free Bi0.5Na0.5TiO3 ceramics under visible light illumination. *J. Am. Ceram. Soc.* 2021, *104*, 4033−4040.

(16) Lv, X. J.; Dong, S.; Huang, X.; Cao, B.; Zeng, S. X.; Wang, Y. J.; Wu, T.; Chen, L.; Wang, J. L.; Yuan, G. L.; Liu, J. M. Giant Bulk Photostriction and Accurate Photomechanical Actuation in Hybrid Perovskites. *Adv. Opt. Mater.* 2021, *9*, No. 2100837.

(17) Tsai, H.; Asadpour, R.; Blancon, J.-C.; Stoumpos, C. C.; Durand, O.; Strzalka, J. W.; Chen, B.; Verduzco, R.; Ajayan, P. M.; Tretiak, S.; Even, J.; Alam, M. A.; Kanatzidis, M. G.; Nie, W.; Mohite, A. D. Light-induced lattice expansion leads to high-efficiency perovskite solar cells. *Science* 2018, *360*, 67−70.

(18) Zheng, F.; Tan, L. Z.; Liu, S.; Rappe, A. M. Rashba spin−orbit coupling enhanced carrier lifetime in CH3NH3PbI3. *Nano Lett.* 2015, *15*, 7794−7800.

(19) Parrott, E. S.; Milot, R. L.; Stergiopoulos, T.; Snaith, H. J.; Johnston, M. B.; Herz, L. M. Effect of structural phase transition on charge-carrier lifetimes and defects in CH3NH3SnI3 perovskite. *J. Phys. Chem. Lett.* 2016, *7*, 1321−1326.

(20) Gottesman, R.; Gouda, L.; Kalanoor, B. S.; Haltzi, E.; Tirosh, S.; Rosh-Hodesh, E.; Tischler, Y.; Zaban, A.; Quarti, C.; Mosconi, E.; de Angelis, F. Photoinduced reversible structural transformations in free-standing CH3NH3PbI3 perovskite films. *J. Phys. Chem. Lett.* 2015, *6*, 2332−2338.

(21) Wu, X.; Tan, L. Z.; Shen, X.; Hu, T.; Miyata, K.; Trinh, M. T.; Li, R.; Coffee, R.; Liu, S.; Egger, D. A.; Makasyuk, I.; Zheng, Q.; Fry, A.; Robinson, J. S.; Smith, M. D.; Guzelturk, B.; Karunadasa, H. I.; Wang, X.; Zhu, X.; Kronik, L.; Rappe, A. M.; Lindenberg, A. M. Light-induced picosecond rotational disordering of the inorganic sublattice in hybrid perovskites. *Sci. Adv.* 2017, *3*, No. e1602388.

(22) Zhou, Y.; You, L.; Wang, S.; Ku, Z.; Fan, H.; Schmidt, D.; Rusydi, A.; Chang, L.; Wang, L.; Ren, P.; Chen, L.; Yuan, G.; Chen, L.; Wang, J. Giant photostriction in organic−inorganic lead halide perovskites. *Nat. Commun.* 2016, *7*, 11193.

(23) Wei, T. C.; Wang, H. P.; Li, T. Y.; Lin, C. H.; Hsieh, Y. H.; Chu, Y. H.; He, J. H. Photostriction of CH3NH3PbBr3 perovskite crystals. *Adv. Mater.* 2017, *29*, No. 1701789.

(24) Photostrictive Actuators. *J. Jpn. Soc. Precis. Eng.* 1992, *58* (), 419−421, DOI: 10.2493/jjspe.58.419.

(25) Sun, D.; Tong, L. Modeling of wireless remote shape control for beams using nonlinear photostrictive actuators. *Int. J. Solids Struct.* 2007, *44*, 672−684.

(26) Datskos, P. G.; Rajic, S.; Sepaniak, M. J.; Lavrik, N.; Tipple, C. A.; Senesac, L. R.; Datskou, I. Chemical detection based on adsorption-induced and photoinduced stresses in microelectromechanical systems devices. *J. Vac. Sci. Technol. B* 2001, *19*, 1173−1179.

(27) Rolston, N.; Bennett-Kennett, R.; Schelhas, L. T.; Luther, J. M.; Christians, J. A.; Berry, J. J.; Dauskardt, R. H. Comment on "Light-

induced lattice expansion leads to high-efficiency perovskite solar cells". *Science* **2020**, *368*, No. eaay8691.

(28) Kundys, B. Photostrictive materials. *Appl. Phys. Rev.* **2015**, *2*, No. 011301.

(29) Burkert, F.; Kreisel, J.; Kuntscher, C. A. Optical spectroscopy study on the photo-response in multiferroic BiFeO3. *Appl. Phys. Lett.* **2016**, *109*, No. 182903.

(30) Miao, X.; Qiu, T.; Zhang, S.; Ma, H.; Hu, Y.; Bai, F.; Wu, Z. Air-stable CsPb 1− x Bi x Br 3 (0≤ x≪ 1) perovskite crystals: Optoelectronic and photostriction properties. *J. Mater. Chem. C* **2017**, *5*, 4931−4939.

(31) Xue, J.; Yang, D. D.; Cai, B.; Xu, X. B.; Wang, J.; Ma, H.; Yu, X. C.; Yuan, G. L.; Zou, Y. S.; Song, J. Z.; Zeng, H. B. Photon-Induced Reversible Phase Transition in CsPbBr3 Perovskite. *Adv. Funct. Mater.* **2019**, *29*, No. 1807922.

(32) Bergamini, L.; Sangiorgi, N.; Gondolini, A.; Sanson, A. CsPbBr3 for photoelectrochemical cells. *Solar Energy* **2020**, *212*, 62−72.

(33) Protesescu, L.; Yakunin, S.; Bodnarchuk, M. I.; Krieg, F.; Caputo, R.; Hendon, C. H.; Yang, R. X.; Walsh, A.; Kovalenko, M. V. Nanocrystals of Cesium Lead Halide Perovskites (CsPbX3, X = Cl, Br, and I): Novel Optoelectronic Materials Showing Bright Emission with Wide Color Gamut. *Nano Lett.* **2015**, *15*, 3692−3696.

(34) Kresse, G.; Furthmüller, J. Efficient iterative schemes for ab initio total-energy calculations using a plane-wave basis set. *Phys. Rev. B* **1996**, *54*, 11169−11186.

(35) Perdew, J. P.; Chevary, J. A.; Vosko, S. H.; Jackson, K. A.; Pederson, M. R.; Singh, D. J.; Fiolhais, C. Atoms, molecules, solids, and surfaces: Applications of the generalized gradient approximation for exchange and correlation. *Phys. Rev. B* **1992**, *46*, 6671.

(36) Enkovaara, J.; Rostgaard, C.; Mortensen, J. J.; Chen, J.; Dułak, M.; Ferrighi, L.; Gavnholt, J.; Glinsvad, C.; Haikola, V.; Hansen, H.; Kristoffersen, H. H.; Kuisma, M.; Larsen, A. H.; Lehtovaara, L.; Ljungberg, M.; Lopez-Acevedo, O.; Moses, P. G.; Ojanen, J.; Olsen, T.; Petzold, V.; Romero, N. A.; Stausholm-Møller, J.; Strange, M.; Tritsaris, G. A.; Vanin, M.; Walter, M.; Hammer, B.; Häkkinen, H.; Madsen, G. K. H.; Nieminen, R. M.; Nørskov, J. K.; Puska, M.; Rantala, T. T.; Schiøtz, J.; Thygesen, K. S.; Jacobsen, K. W. Electronic structure calculations with GPAW: a real-space implementation of the projector augmented-wave method. *J. Phys. Condens. Matter* **2010**, *22*, No. 253202.

(37) Maintz, S.; Deringer, V. L.; Tchougréeff, A. L.; Dronskowski, R. LOBSTER: A tool to extract chemical bonding from plane-wave based DFT. *J. Comput. Chem.* **2016**, *37*, 1030.

(38) Stoumpos, C. C.; Malliakas, C. D.; Peters, J. A.; Liu, Z. F.; Sebastian, M.; Im, J.; Chasapis, T. C.; Wibowo, A. C.; Chung, D. Y.; Freeman, A. J.; Wessels, B. W.; Kanatzidis, M. G. Crystal Growth of the Perovskite Semiconductor CsPbBr3: A New Material for High-Energy Radiation Detection. *Cryst. Growth Des.* **2013**, *13*, 2722−2727.

(39) Du, K. Z.; Wang, X. M.; Han, Q. W.; Yan, Y. F.; Mitzi, D. B. Heterovalent B-Site Co-Alloying Approach for Halide Perovskite Bandgap Engineering. *ACS Energy Lett.* **2017**, *2*, 2486−2490.

(40) Lu, Y.-B.; Cong, W.-Y.; Guan, C.; Sun, H.; Xin, Y.; Wang, K.; Song, S. Light enhanced moisture degradation of perovskite solar cell material CH 3 NH 3 PbI 3. *J. Mater. Chem. A* **2019**, *7*, 27469−27474.

(41) Lu, Y.-B.; Kong, X.; Chen, X.; Cooke, D. G.; Guo, H. Piezoelectric scattering limited mobility of hybrid organic-inorganic perovskites CH3NH3PbI3. *Sci. Rep.* **2017**, *7*, 41860.

(42) Wu, Q. Q.; Li, J. P.; Xue, S. M.; Zhao, Y. T.; Liu, F. C.; Huo, Q. H.; Mi, J.; Guan, C. B.; Cong, W. Y.; Lu, Y. B.; Ren, J. F. Bandgap Engineering of Cesium Lead Halide Perovskite CsPbBr3 through Cu Doping. *Adv. Theory Simul.* **2022**, *5*, No. 2200190.